AFRL-AFOSR-VA-TR-2020-0068

Grain and Interface Engineering for High Efficiency Hybrid Perovskite Solar Cells

Jeffrey Shield
UNIVERSITY OF NEBRSKA

03/29/2020
Final Report

Air Force Research Laboratory
AF Office Of Scientific Research (AFOSR)/ RTB2
Arlington, Virginia 22203
Air Force Materiel Command

REPORT DOCUMENTATION PAGE

Form Approved
OMB No. 0704-0188

1. REPORT DATE *(DD-MM-YYYY)*	2. REPORT TYPE	3. DATES COVERED *(From - To)*
22-06-2020	Final Performance	15 May 2016 to 14 Feb 2020

4. TITLE AND SUBTITLE
Grain and Interface Engineering for High Efficiency Hybrid Perovskite Solar Cells

5a. CONTRACT NUMBER

5b. GRANT NUMBER
FA9550-16-1-0299

5c. PROGRAM ELEMENT NUMBER
61102F

6. AUTHOR(S)
Jeffrey Shield

5d. PROJECT NUMBER

5e. TASK NUMBER

5f. WORK UNIT NUMBER

7. PERFORMING ORGANIZATION NAME(S) AND ADDRESS(ES)
UNIVERSITY OF NEBRSKA
151 Whittier Research Center 2200 Vine St
LINCON, NE 68583 US

8. PERFORMING ORGANIZATION REPORT NUMBER

9. SPONSORING/MONITORING AGENCY NAME(S) AND ADDRESS(ES)
AF Office of Scientific Research
875 N. Randolph St. Room 3112
Arlington, VA 22203

10. SPONSOR/MONITOR'S ACRONYM(S)
AFRL/AFOSR RTB2

11. SPONSOR/MONITOR'S REPORT NUMBER(S)
AFRL-AFOSR-VA-TR-2020-0068

12. DISTRIBUTION/AVAILABILITY STATEMENT
A DISTRIBUTION UNLIMITED: PB Public Release

13. SUPPLEMENTARY NOTES

14. ABSTRACT
The goal of this project is to overcome challenges regarding the fabrication of high-efficiency hybrid perovskite photovoltaic planar heterojunction (PHJ) devices using a low-temperature solution process. Challenges that will be addressed include the 1) presence of too many non-radiative charge recombination channels and 2) lack of proper charge transport layers in PHJ devices. Our approach to address these challenges is to form compact highly crystalline organometal trihalide perovskite films with a large grain aspect ratio by the interdiffusion of solution-deposited lead iodine and methylammonium halide stacking precursor layers, and modify the anode and cathode with functional charge transport layers to eliminate the charge recombination channels.

15. SUBJECT TERMS
hybrid perovskite, solution processable solar cells, grain boundary control

16. SECURITY CLASSIFICATION OF:			17. LIMITATION OF ABSTRACT	18. NUMBER OF PAGES	19a. NAME OF RESPONSIBLE PERSON
a. REPORT	b. ABSTRACT	c. THIS PAGE			CASTER, KENNETH
Unclassified	Unclassified	Unclassified	UU		19b. TELEPHONE NUMBER *(Include area code)* 703-588-8487

Grain and Interface Engineering for High Efficiency Hybrid Perovskite Solar Cells

Air Force Office of Scientific Research (AFOSR)

Grant FA9550-16-1-0299 Final Performance Report

Project title: Material and Interface Engineering for High Efficiency Planar Heterojunction Hybrid Perovskite Solar Cells

PI: Jeffry Shield, Professor,

Department of Mechanical and Materials Engineering

University of Nebraska Lincoln

Phone: (402) 472-2378

Email: jshield@unl.edu

Co-PI: Jinsong Huang, Professor,

Department of Applied Physical Science

University of North Carolina Chapel Hill

Phone: (919) 445-1107

Email: jhuang@unc.edu

Program Manager: Dr. Kenneth C. Caster, Program Officer, Organic Materials Chemistry

Air Force Office of Scientific Research (AFOSR)

Arlington, VA

kenneth.caster@us.af.mil

703-588-8487

I. Summary: Objectives and Status of Effort

The goal of this project is to overcome challenges regarding the fabrication of high-efficiency hybrid perovskite photovoltaic planar heterojunction devices using a low-temperature solution process. Our approach to address these challenges is to form compact highly crystalline hybrid perovskite films with a large grain aspect ratio by the interdiffusion of solution-deposited lead iodine and methylammonium halide stacking precursor layers, and modify the anode and cathode with functional charge transport layers to eliminate the charge recombination channels. In addition, we focused on the passivation and stabilization of perovskite surfaces and grain boundaries, which are weakest locations in perovskite films, to enhance not only the efficiency of hybrid perovskite solar cells, but also stability. We explored at least 20 type of organic passivation molecules, and carefully studied their passivation mechanism, and designed new passivation molecules. One notable example is that we proposed to use zwitterions which contain both negative and positive charged function group to passivate defects of positive and negative charged, respectively, which is special to perovskites due to their ionic nature. Another example is to design several ammonic acid molecules to passivate perovskites. In addition to organic passivation molecules, we started a new area of converting the surface of defective perovskite surface into water-insoluble lead oxysalt shell which not only protect perovskite from hazards, but also reduce surface defect density by removing them using chemical reaction. Other strategies such as strengthen the perovskite surface using strong chemical bonding, bilateral amines to bridge defects and grains, etc are developed in this project, which results in record device performance and also greatly deepen the understanding of defects in hybrid perovskites.

II. Accomplishments

1. Understanding the function of fullerenes

Results are published in: *Y. Fang, C. Bi, D. Wang, and J. Huang*, The Functions of Fullerenes in Hybrid Perovskite Solar Cells, ACS Energy Letters, Invited Perspective, 2, 782-794 (2017)*

How do fullerenes reduce current hysteresis?

Current – voltage hysteresis, i.e., the scan direction dependent non-overlapping current – voltage curves, has been widely observed in non-optimized perovskite solar cells. We reported the first hysteresis-free perovskite solar cells by using fullerenes as ETL. The perovskite solar cells with fullerenes usually exhibited less or no hysteresis in comparison to those with TiO_2 as ETL. After a couple of years' studies world widely, it slowly comes to a consensus that the origins of current hysteresis are charge traps or interfacial polarization, while in the latter case the polarization is caused by either ion migration or interfacial charge accumulation. Therefore the fullerenes have to overcome all these possible channels that all cause current hysteresis.

What is the function of double-fullerene layers?

It is worth noting that the combination of PCBM and C_{60} double-fullerene layers is found by us to be always necessary to achieve the highest efficiency, in addition to eliminating the current hysteresis. The spun fullerenes (either C_{60} or other derivatives) form the conformal covering layer on the perovskite film surfaces to fill possible pin-holes, while the thermal evaporated fullerene can further cover the pin-holes in the first fullerene layer, which effectively eliminates the leakage current. In addition, PCBM and C_{60} were shown to have different but complementary trap passivation capability. The devices with PCBM/C_{60} double fullerene layer show better trap passivation effect than those with only one type of fullerene layer.

Does the doping of fullerene by perovskite contribute to the eliminated photocurrent hysteresis at room temperature?

The discovery of enhanced conductivity of PCBM by blending with precursor MAI raised one question whether it is the dominating mechanism in eliminating the current hysteresis by efficiently collecting charge. In fact, the doping of fullerenes by iodine containing molecules have been previously developed for highly conductive fullerene materials. We actually took advantage of this doping effect to enhance the conductivity of a low mobility fullerene derivative to reduce the contact resistance and enhance the device fill factors. However, its contribution to hysteresis reduction might not be significant for the following reasons. First of all, an increased series resistance in any type of solar cells will only change the device efficiency, but should not cause a hysteresis. Second, one would argue that if the low conductivity of the charge transport layers is the origin of current hysteresis, it would already be easily eliminated by using much more conductive metal electrodes, which is however not the case. Third, the doping induced conductivity enhancement of fullerenes usually increases carrier concentration, while the charge extraction relies more on the mobility of the fullerene layer. Finally, one may also argue the dynamic doping and de-doping of fullerene induced by ion diffusion could cause a dynamic variation of the series resistance in the fullerene layer, which may cause the hysteresis. A simple calculation of the fullerene conducitivity shows that it won't induce notable resistivity and voltage loss during the current scanning, once its thickness is small enough (<20 nm). In addition, removing fullerene should have eliminated this hysteresis origin, which is however opposite to the experimental observations. For the same token, the doping of poly(3,4-ethylenedioxythiophene) polystyrene sulfonate (PEDOT:PSS) by the perovskite should not play an major role in reducing hysteresis in perovskite solar cells, because hole transport layers (HTL) with much lower conductivity, such as poly[bis(4-phenyl)(2,4,6-trimethylphenyl)amine (PTAA), won't cause hysteresis either. As long as the PTAA layer thickness is small enough, its conductivity does not limit the efficiency of perovskite solar cells either, even without any doping.

Why do some perovskite/fullerene solar cells still have hysteresis at low temperature?

Recently, *Durrant* and his colleagues discovered an interesting phenomenon that the perovskite solar cells with PCBM as cathode exhibited apparent hysteresis at low temperature,

even if they were hysteresis-free at room temperature. The ion-migration issue could be ruled out as the origin of the hysteresis at low temperature, since the ion migration should be frozen at low temperature. We speculate that one possible reason to explain this phenomenon is that fullerenes might be more effective in passivating the deep traps on the perovskite film surface; while the unpassivated shallow traps, which do not affect the carrier transport at room temperature due to thermal activation, could behave as "deep traps" at low temperature. These shallower traps can be still too deep for the trapped carriers to escape, because the thermal activation energy, k_BT, is much smaller at lower temperature. And therefore the consequent slow trapping and detrapping events would cause the hysteresis. In this context, we can estimate the "shallower-traps" have an energy depth in the range of tens of meV. In many cases, the measured exciton binding energies derived from temperature dependent photoluminescence and absorption spectra are in this range, which indicates they may have the same origin of energy disorder, and the excitons are dominantly bound excitons, rather than free excitons.

Is perovskite:PCBM blend a bulk heterojunction?

Very high fill factors of 80%-82% have been achieved recently in PHJ perovskite solar cells with fullerene intentionally incorporated in precursor solution so that fullerenes can be incorporated at the grain boundaries. One scenario was put out that the fullerene intergranular layers act as electron transport channel, making the perovskite solar cells resemble BHJ based organic solar cells. The BHJ structure is required in efficient organic solar cells, because the exciton diffusion length in organic semiconductor materials is much less than the optical absorption length. Fullerenes are introduced to form BHJ with other p-type polymers to facilitate exciton separation and electron transportation.

There is still no direct evidence for the formation of fullerene percolation network along the grain boundaries, which will need further study from morphology characterization. On the other hand, even if the fullerene intergranular layers formed percolation network, it is questionable whether electrons will go through the fullerene intergranular layer in perovskite solar cells. Perovskite materials have reported hole and electron mobility in range from 6 cm^2/Vs to 200 cm^2/Vs depending on the chemical composition and crystallinity, which are remarkably high for solution-processed semiconductors, while fullerenes generally have 3-5 orders magnitude lower mobility of 10^{-4}-10^{-3} cm^2/Vs. It is difficult for electrons to choose the much lower mobility channels. Herein, we use a simple design of light emitting diode (LED) to demonstrate the much better charge mobility in perovskite materials and much faster drift of carrier through the perovskite layer than organic charge transport layers. As illustrated in **Figure 1**, we fabricated LED devices with a structure of ITO/PTAA/$MAPbCl_xBr_{3-x}$/ Bathophenanthroline (Bphen)/Al. The PTAA layer served as hole injection layer as well as electron blocking layer, while Bphen layer served as electron injection and hole blocking layer. The design was aimed to make perovskite LED by confining electrons and holes in the perovskite layer for radiative recombination. However, the device showed sky blue electroluminescence with a peak at 500 nm, which actually came from the emission of PTAA layer. This result can be explained by the fact that the electron transport time through the perovskite layer is much shorter than hole transport time through the PTAA layer. Thus the electrons go through the perovskite layer and recombined with the holes within the PTAA

layer. Considering the hole mobility in PTAA measured by space-charge-limited-current method is 10^{-3}-10^{-2} cm^2/Vs, which is comparable or slightly larger than electron mobility in regular fullerene materials, the solution processed perovskite thin films should possess an electron mobility much larger than this value.

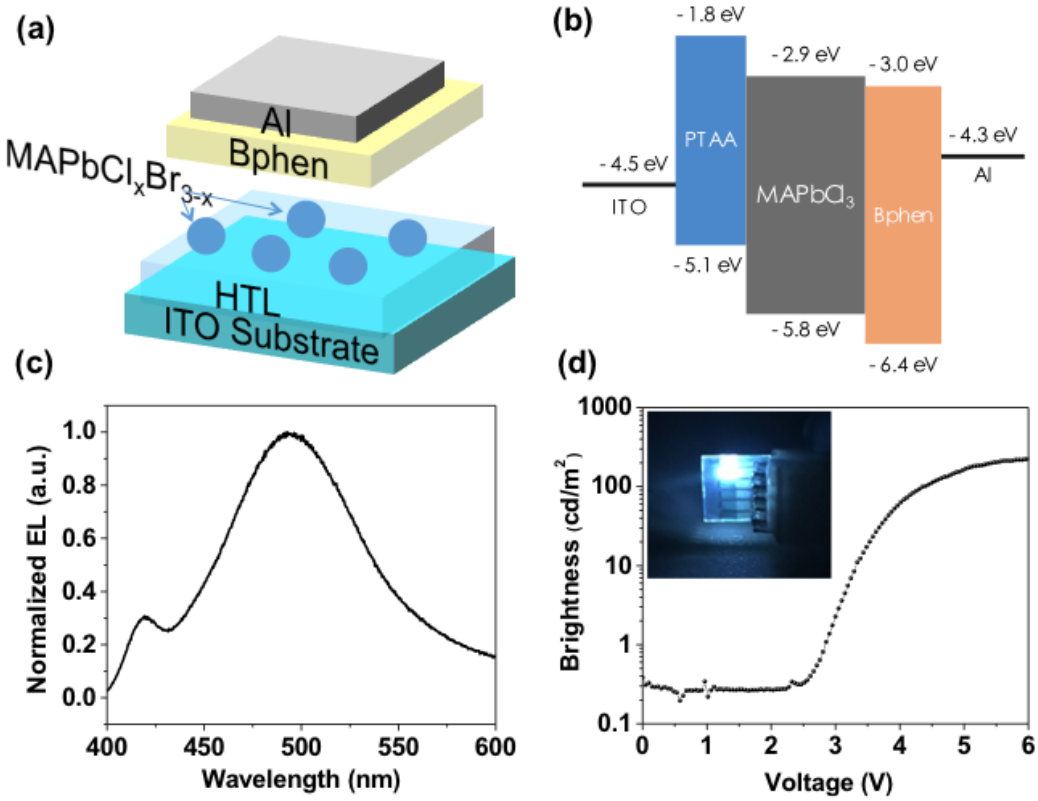

Figure 1 *(a) Device structure of the perovskite based LED; (b) Band diagram of the perovskite based LED; (c) Normalized electroluminescence under a bias of 6 V; (d) The brightness of the device under different bias. Insert is the photo image of the device at 6 V.*

Recent ultrafast photodetector study with transient photocurrent (TPC) measurement reveals the very fast electron extraction in the regular perovskite solar cells. With a regular solar cell structure of ITO/PTAA/$MAPbI_3$/C_{60}/Bathocuproine (BCP)/Cu (Device type 1), we showed that photo-generated electrons could be extracted out of the solar cells by the built-in electric field at short circuit condition in sub-nanosecond after generation (**Figure 2a**). A time-resolved photoluminescence system was actually constructed with the perovskite photodetectors. We also followed the method reported by *Chiang et al.* to intentionally incorporate PCBM into the grain boundaries (Device type II). An electron transit time of 4.9 ns was recorded, which is limited by the rising time (4 ns) of pulse laser used here. When we measured the device type I with this pulse laser, we got similar response time of 4 ns. Such fast response speed is barely possible if electrons go through the fullerene intergranular layer (**Figure 2c**). A simple calculation of electron transit time through PCBM intergranular layer across a thickness of 500 nm is around 360-3600 ns with a mobility of 10^{-3}-10^{-2} cm^2/Vs. A final question comes up on whether intergranular fullerenes will

still accept electrons since it does quench photoluminescence of perovskite. We would argue that it is a competition process for electron extraction through perovskite and electron transfer to fullerene. The thickness of the intergraluar fullerene layer is around 1-3 nm if it is added after perovskite film formation, which is defined by grain boundaries geometry. While photogenerated electrons affinity to intergranular fullerenes may still transfer to fullerenes, most of photogenerated electrons would be quickly collected by the built-in field through perovskites with grain size much larger than the electron transfer distance. In case of fullerenes are randomly distributed in perovskite grain boundaries without forming percolation path, the fullerene clusters may still accept some electrons but will act as electron traps.

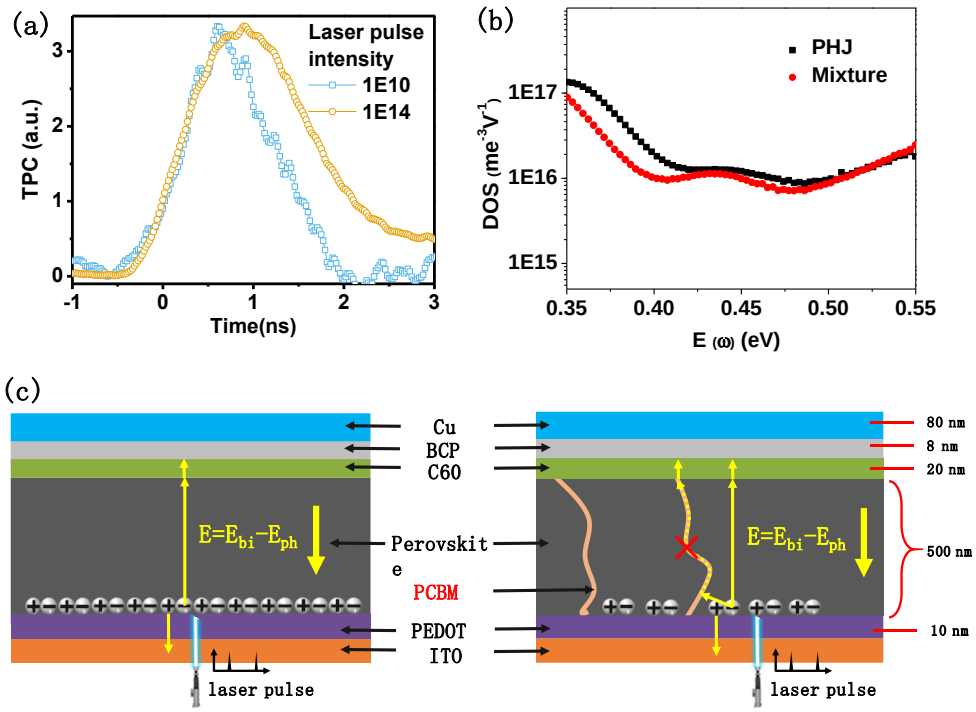

Figure 2 *(a) Transient photocurrent curves of perovskite photodiode. (b)Trap density in fullerene/perovskite PHJ and Mixture devices obtained by TAS measurement. (c) Schematic diagram of the electron transport pathway in fullerene/perovskite PHJ and Mixture devices.*

We thus conclude that the fullerene layer between grain boundaries plays a major role of passivating the defects, which reduces the charge recombination at grain boundaries and increases the fill factor. It is confirmed by our measurement that $MAPbI_3$:PCBM mixture device had a slightly lower trap density than PHJ device (**Figure 2b**). In this context, other non-conducting materials can replace fullerenes, if they can also passivate the defects on the surface of perovskite films, and its thickness is small enough so that charge can tunnel through to electrode. Nevertheless, another important function of the fullerene layer is to separate the perovskite from the electrodes to prevent the damage of perovskite during the deposition of electrodes. So completely replacing fullerene layers by other function layers needs to consider all these functions of fullerene layers.

2. Dual Passivation of the Cationic and Anionic Defects in Hybrid Perovskites with Quaternary Ammonium Halides

Results are published in: Xiaopeng Zheng, Bo Chen, Jun Dai, Yanjun Fang, Yang Bai, Yuze Lin, Haotong Wei, Xiao Cheng Zeng and Jinsong Huang, Defect passivation in Hybrid Perovskite Solar Cells using Quaternary Ammonium Halides Anions and Cations, Nature Energy, 2, 17102, 2017

The ionic nature of OIHP materials imposes different requirement for the defects passivation with covalent-bonding semiconductors such as silicon (Si). The passivation of Si is mainly achieved by the elimination of the Si dangling bonds by formation of Si-O, Si-N or Si-H covalent bonds, which is however not applicable to strong ionic OIHPs. So far different passivation molecules have been reported to perform as electron donors or electron acceptors that can interact with the charged defects of OIHPs, and thereafter annihilate the relevant defect-induced charge traps. Lewis acids, such as phenyl-C61-butyric acid methyl ester (PCBM), as the good electron transporting materials could accept an electron from the negative charged Pb-I antisite defects PbI_3^- or under-coordinated halide ions and thus passivate the halide-induced deep traps. Lewis base molecules, such as thiophene or pyridine, usually perform as the electron donors which could bind to the positively charged under-coordinated Pb^{2+} ions. However, most of these passivation molecules could only passivate one type of defects, either positive charged or negative charged defects. The defects in OIHP materials are charged, either positively or negatively, and therefore the passivation of them should take the charge neutrality into consideration.

We designed a new system of materials, quaternary ammonium halides (QAHs), to passivate both cationic and anionic defects in OIHP with its negative- and positive- charged components. The planar heterojunction perovskite solar cells in this study were structured as poly[bis(4-phenyl)(2,4,6-trimethylphenyl)amine] (PTAA)/$CH_3NH_3PbI_3$/functional layer/ fullerene (C_{60})/ 2,9-dimethyl-4,7-diphenyl-1,10-phenanthroline (BCP)/copper (Cu), as shown in **Figure 3a**. **Figure 3b** illustrated the passivation mechanism. In our previous studies, the fullerene derivative phenyl-C61-butyric acid methyl ester (PCBM) is used as perovskite passivation material which is used for control device here. With an initial objective to enhance their moisture stability, we replaced PCBM by amphiphilic molecules with different functional groups, including of L-α-Phosphatidylcholine, Tween-20, and Polyethylene-block-poly(ethylene glycol) (PE-PEG) whose chemical structures are shown in **Figure 3**c. Our in-parallel studies showed that converting the surface of electron transport layer into hydrophobic could enhance the water resistance of the perovskite films and device stability in moisture. The application of amphiphilic materials was designed to attach them to the perovskite layer with the hydrophilic side, and expose the hydrophobic side to air.

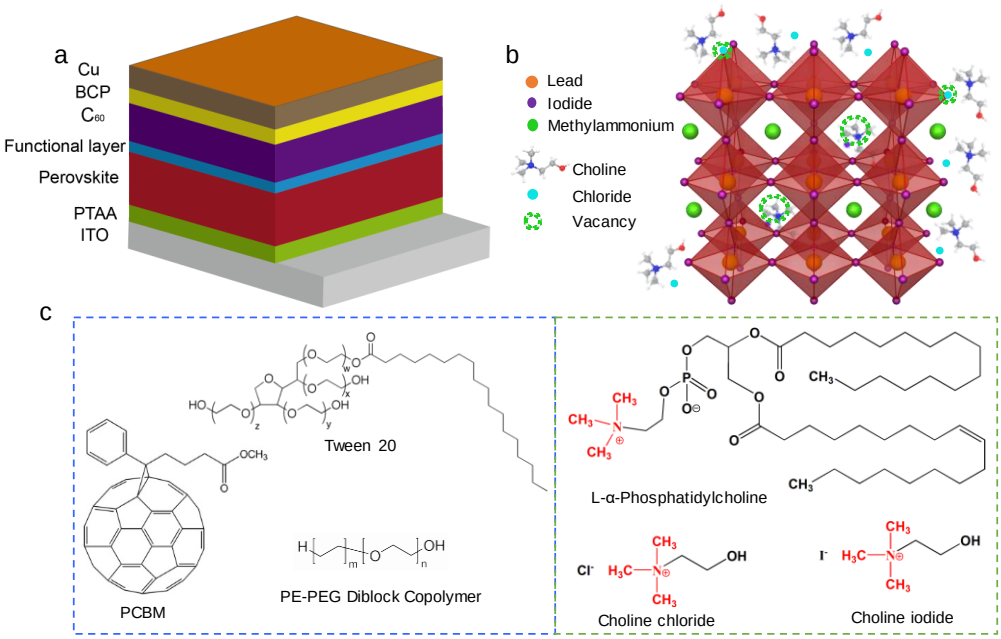

Figure 3. Device structure and the passivation mechanism by quaternary ammonium halides (QAHs). ***a***, *The device structure of perovskite planar heterojunction solar cells.* ***b***, *Schematic illustration of QAHs assembled on the defect sites.* ***c***, *Chemical structures of phenyl-C61-butyric acid methyl ester (PCBM), Tween 20, Polyethylene-block-poly(ethylene glycol) (PE-PEG), L-α-Phosphatidylcholine, Choline iodide, and Choline chloride.*

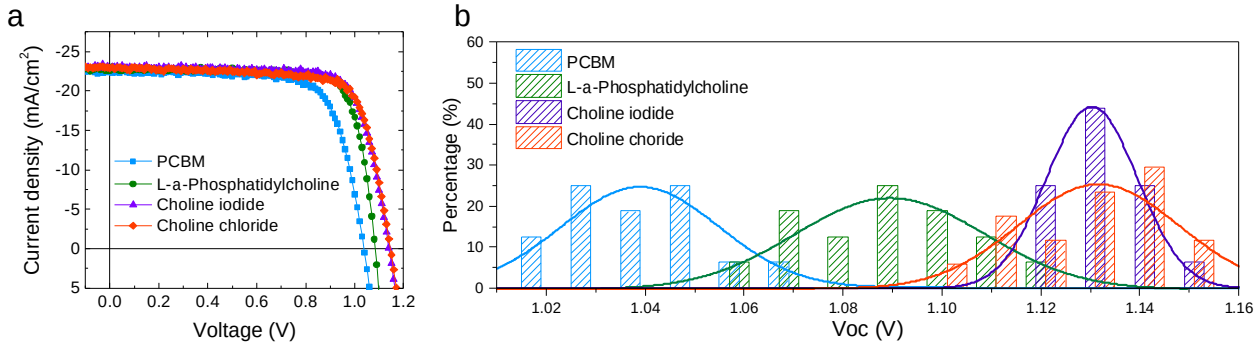

Figure 4 a, *Current density-voltage (J-V) characteristics of two-step processed $MAPbI_3$ devices with different passivation layers.* ***b***, *The statistics of V_{OC} distribution for devices with PCBM, L-α-Phosphatidylcholine, Choline iodide, and Choline chloride. (Statistic from 64 samples). The solid lines represent the Gauss distribution fitting for the statistic of V_{OC}.*

Figure 4a shows the current density-voltage (*J-V*) curves of the $MAPbI_3$ devices with deposition of different passivation layers. The control device with PCBM layer showed typical performance with a short circuit current density (J_{SC}) of 22.5 $mAcm^{-2}$, a V_{OC} of 1.04 V, a fill factor (FF) of 73.0%, and a PCE of 17.1%. Compared to the device with PCBM layers, the performances of the $MAPbI_3$ devices with Tween, and PE-PEG buffer layers were even worse with maximum

PCE between 13.6 % and 15.5%, even after we optimized the concentration of Tween and PE-PEG solution. It indicates that Tween and PE-PEG cannot passivate the surface defects on $MAPbI_3$. In striking contrast, the devices with L-α-Phosphatidylcholine layer showed a significantly improved performance with an average J_{SC} of 22.7 mA cm^{-2}, V_{OC} of 1.08 V, FF of 80.0%, and PCE of 19.6%. The performance enhancement and hysteresis-free behavior were tentatively attributed to the passivation effect of L-α-Phosphatidylcholine molecules.

The distinct performance led us to think about what is unique about L-α-Phosphatidylcholine molecule in passivating $MAPbI_3$. In comparison to Tween and PE-PEG, L-α-Phosphatidylcholine has the same long alkyl chain, while the difference is that L-α-Phosphatidylcholine has choline phosphate zwitterion structure. So we speculate that its zwitterion structure with the choline group passivates $MAPbI_3$. To verify it, we used two other choline zwitterion molecules, also known as quaternary ammonium halides (QAHs), including choline iodide and choline chloride which have no long alkyl chain, as the interfacial layer. The V_{OC} of the perovskite devices was significantly increased by choline iodide and choline chloride as passivation layers without sacrificing the J_{SC} and FF of the devices, which confirmed our speculation. The devices with choline iodide and choline chloride showed higher V_{OC} of 1.14 and 1.15 V. Consequently, PCEs of the $CH_3NH_3PbI_3$ devices with choline iodide and choline chloride passivation layers were increased to 20.1%, and 20.0%, respectively. **Figure 4b** shows the V_{OC} distribution of the devices with different passivation layers. The average V_{OC} values are 1.04, 1.09, 1.13, and 1.13 V for the statistic V_{OC} of the devices with PCBM, L-α-Phosphatidylcholine, choline iodide and choline chloride, respectively. The larger average V_{OC} of the devices passivated by QAHs than by L-α-Phosphatidylcholine indicates there is additional passivation effect from the halide ions, because both of them have the quaternary ammonium component. There are both positively-charged cationic and negatively-charged anionic defects in OIHPs, such as I^- and MA^+ vacancies, respectively, while quaternary ammonium ions are expected to only passivate MA^+ vacancies by occupying cuboctahedral sites to compensate the MA^+ loss on the film surfaces, as illustrated in **Figure 3b**. Loss of halide ions by the evaporation of MAI during thermal annealing process needs to be compensated by additional halide ions. Therefore, the dual passivation effect is critical in achieving the high efficiency device reported here. The notable better passivation effect of choline chloride than choline iodide can be explained by the stronger Pb-Cl bonding than Pb-I bond, and small amount of Cl addition has been broadly reported to enhance the charge recombination lifetime in $MAPbI_3$. Based on the mechanism of passivation presented here, any Zwitterion molecular structure should have good passivation effect, because they have both negative and positive electric charges. A Zwitterion molecule may passivate both cationic and anion defects if the spacing of these defects happens to be the same with the size of the Zwitterion molecule. However, the defects at the surface of perovskite films may have very complicated distribution and compositions. The positive and negative charge defects may distribute away from each other, and their ratio may not be 1:1, because the perovskite film surface does not necessarily reach thermal dynamic stable states right after annealing processing, and the surfaces defects may pair up with bulk defects. In this context, the QAH molecule with separated positive and negative

ions have the advantage of self-adaptive selection of defects with opposite charges for passivation, which is not limited by the complicated surface defect composition or distribution.

For the $FA_{0.83}MA_{0.17}Pb(I_{0.83}Br_{0.17})_3$ perovskite films made by one-step anti-solvent methods, choline chloride passivation could also greatly improve the photovoltaic performance. The best PCE of 21.0 % was achieved by choline chloride passivated $FA_{0.85}MA_{0.15}Pb(I_{0.85}Br_{0.15})_3$ with a J_{SC} of 23.7 mA/cm^2, V_{OC} of 1.13-1.14 V, and FF of 78.0 % under forward and reverse scanning with negligible hysteresis, as shown in **Figure 5a**. The performance of the device under forward and reverse scanning is shown in Table in **Figure 5b**. We speculate the passivation by coating of the choline chloride layer should also enhance the stability of the perovskite films in ambient environment, because the healing of the defective sites on the film surface should inhibit the permeation of moisture and oxygen through the defects. To verify this, the stability of $FA_{0.83}MA_{0.17}Pb(I_{0.83}Br_{0.17})_3$ devices with choline chloride and L-α-Phosphatidylcholine functional layers were monitored by putting the unencapsulated devices in ambient atmosphere at room temperature and relative humidity of 50%-85%, and the device performance are summarized in **Figure 5c**. The devices with choline chloride layers retained almost 100% of the initial PCEs after the storage in the ambient condition for over one month. Interestingly, the V_{OC} of the devices increased during the first 5 days of storage in both types of devices with choline chloride passivation. The L-α-Phosphatidylcholine modified devices showed inferior performance, 30% loss of the initial PCE after 800 h storage in the ambient condition, despite that the long hydrophobic alkane tails could hinder the permeation of moisture. The difference in stability of the devices with two passivation layer highlighted the importance of healing both types of defects.

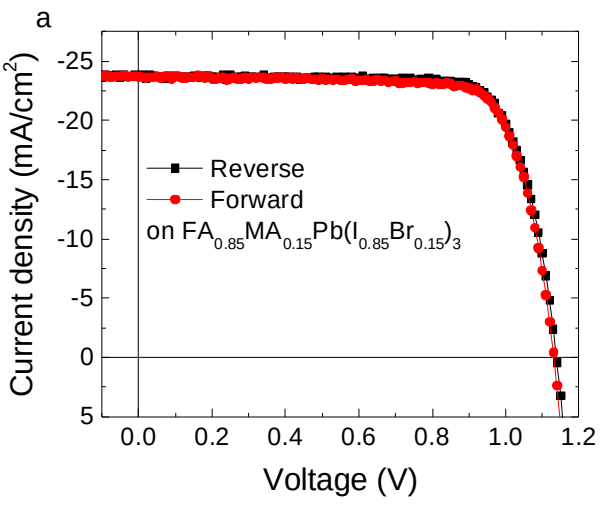

b

	Jsc	Voc	FF	PCE
Reverse	23.7	1.14	78%	21.1%
Forward	23.7	1.13	78%	20.9%

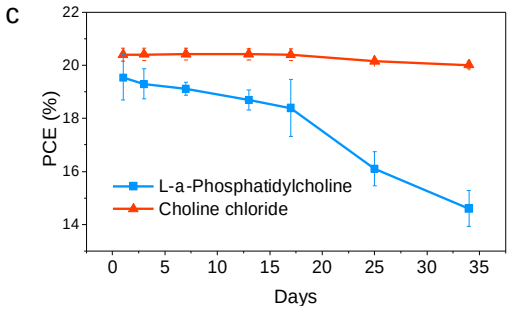

***Figure 5**, **a** J-V curves of the champion device prepared by the Choline Chloride passivation measured in both reverse and forward scanning directions. b summary of device peroformance under forward and reverse scanning. c. Evolution of PCC for the device over 35 days of storage in air. Each average (symbol) and standard deviation (error bar) was calculated from six solar cells.*

The long stability of the unencapsulated devices allows us to certify their efficiency. One of the unencapsulated devices was sent to an accredited independent PV test laboratory (Newport Corporation PV Lab, Montana, USA) for certification. The device with a photomask area of 7.16 mm^2 displayed a certified PCE of 20.59±0.45% and absence of photocurrent hysteresis (**Figure 6**), which represents a record of the time PCE for p-i-n structured OIHP solar cells.

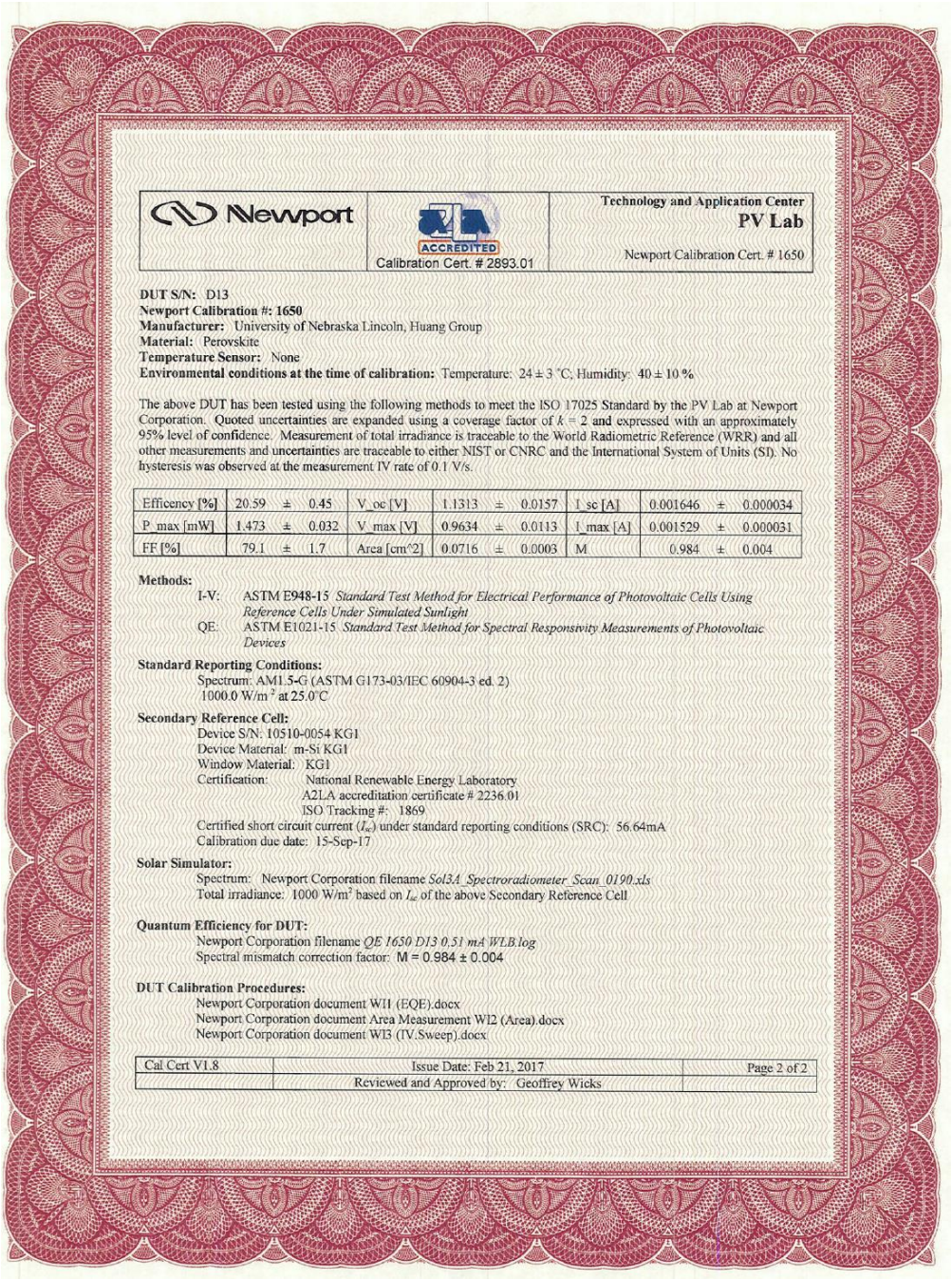

Newport

ACCREDITED
Calibration Cert. # 2893.01

Technology and Application Center
PV Lab
Newport Calibration Cert. # 1650

DUT S/N: D13
Newport Calibration #: 1650
Manufacturer: University of Nebraska Lincoln, Huang Group
Material: Perovskite
Temperature Sensor: None
Environmental conditions at the time of calibration: Temperature: 24 ± 3 °C, Humidity: 40 ± 10 %

The above DUT has been tested using the following methods to meet the ISO 17025 Standard by the PV Lab at Newport Corporation. Quoted uncertainties are expanded using a coverage factor of $k = 2$ and expressed with an approximately 95% level of confidence. Measurement of total irradiance is traceable to the World Radiometric Reference (WRR) and all other measurements and uncertainties are traceable to either NIST or CNRC and the International System of Units (SI). No hysteresis was observed at the measurement IV rate of 0.1 V/s.

Efficency [%]	20.59	±	0.45	V_oc [V]	1.1313	±	0.0157	I_sc [A]	0.001646	±	0.000034
P_max [mW]	1.473	±	0.032	V_max [V]	0.9634	±	0.0113	I_max [A]	0.001529	±	0.000031
FF [%]	79.1	±	1.7	Area [cm^2]	0.0716	±	0.0003	M	0.984	±	0.004

Methods:
I-V: ASTM E948-15 *Standard Test Method for Electrical Performance of Photovoltaic Cells Using Reference Cells Under Simulated Sunlight*
QE: ASTM E1021-15 *Standard Test Method for Spectral Responsivity Measurements of Photovoltaic Devices*

Standard Reporting Conditions:
Spectrum: AM1.5-G (ASTM G173-03/IEC 60904-3 ed. 2)
1000.0 W/m^2 at 25.0°C

Secondary Reference Cell:
Device S/N: 10510-0054 KG1
Device Material: m-Si KG1
Window Material: KG1
Certification: National Renewable Energy Laboratory
A2LA accreditation certificate # 2236.01
ISO Tracking #: 1869
Certified short circuit current (I_{sc}) under standard reporting conditions (SRC): 56.64mA
Calibration due date: 15-Sep-17

Solar Simulator:
Spectrum: Newport Corporation filename *Sol3A_Spectroradiometer_Scan_0190.xls*
Total irradiance: 1000 W/m^2 based on I_{sc} of the above Secondary Reference Cell

Quantum Efficiency for DUT:
Newport Corporation filename *QE 1650 D13 0.51 mA WLB.log*
Spectral mismatch correction factor: M = 0.984 ± 0.004

DUT Calibration Procedures:
Newport Corporation document WI1 (EQE).docx
Newport Corporation document Area Measurement WI2 (Area).docx
Newport Corporation document WI3 (IV.Sweep).docx

Cal Cert V1.8	Issue Date: Feb 21, 2017	Page 2 of 2
	Reviewed and Approved by: Geoffrey Wicks	

Figure 6. *Certified device performance by Newport*

3. Argon plasma treatment to tune perovskite surface composition for high efficiency solar cells

Results are published in: *Xun Xiao, Chunxiong Bao, Yanjun Fang, Jun Dai, Benjamin R. Ecker, Yuze Lin, Shi Tang, Ye Liu, Yehao Deng, Xiaopeng Zheng, Yongli Gao, Xiao Cheng Zeng and Jinsong Huang**, Argon plasma treatment to tune perovskite surface composition for high efficiency solar cells and fast photodetectors, *Adv. Mater.*, 30, 1705176. (2018)

The common deep traps on the surface of perovskite films could be complicated, including Pb_i, Pb cluster and I_{MA}. If the organic part, such as MA cation and I anion, could be removed, the I_{MA} might be removed by tune the surface composition, the left lead-rich perovskite surface could be passivated efficiently by known electron transport materials such as fullerenes. Thermal annealing was used to remove MAI to tune the film composition. However, due to the easy decomposition of $MAPbI_3$ under thermal annealing, the decomposition may occurs far below the surface where the charge transport layer cannot reach and thus cause severe charge recombination. We developed an argon plasma treatment (APT) as an effective way to fine tune the surface composition of the perovskite thin films, as illustrated in **Fig. 7**. The APT can effectively remove the organic component of the perovskite surface, which unify the defects type and leave the lead-rich perovskite surface before the deposition of passivating layer for a better passivating effect. The removing of organic component induces an ultra-thin n type self-doping layer, which helps charge extraction by reducing charge trapping at the perovskite film surface. Perovskite solar cells with APT for 2 seconds showed an improved performance with average PCE of 19.3% and best PCE of 20.4%. There still have room to further improve the passivation effect since the PL lifetime is still lower than that of single crystals.

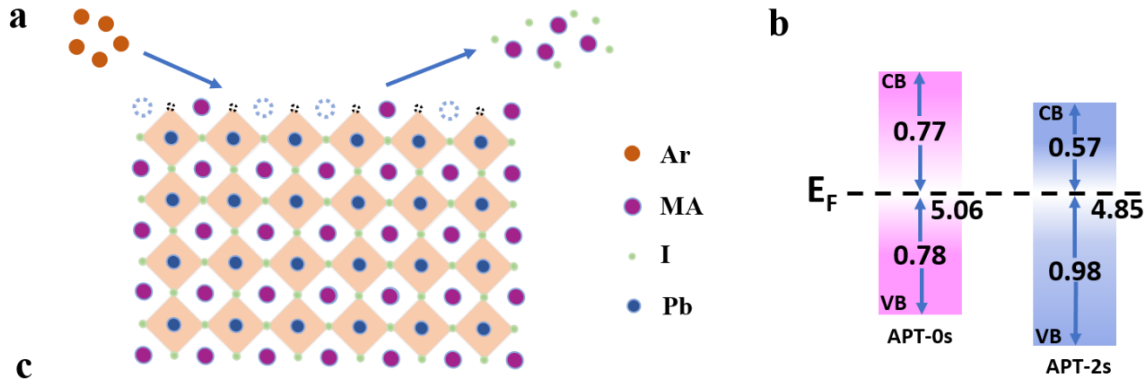

Figure 7. *(a) Scheme of Argon Plasma Treatment (APT) for $MAPbI_3$ surface to remove MAI and expose lead rich surface; (b) UPS measured energetic levels of perovskite surface with APT for 0 s (APT-0s) and 2 s (APT-2s). E_F, CB, and VB represent Fermi level, conductive band and valence band, respectively.;*

4. Hot-substrate Deposition of Hole and Electron Transport Layers for Enhanced Performance in Perovskite Solar Cells

Results are published in: Zhenhua Yu, Linxing Zhang, Sen Tian, Fan Zhang, Bin Zhang, Fangfang

Niu, Pengju Zeng, Junle Qu, Peter Rudd, Jinsong Huang and Jiarong Lian*, Hot-substrate Deposition of Hole and Electron Transport Layers for Enhanced Performance in Perovskite Solar Cells, Adv. Energy Mater., 8, 1701659 (2018).*

Herein, we report a simple hot substrate depostion method to improve the surface morphology of both the hole-transport layer (HTL) of poly(4-butylphenyl-diphenyl-amine) (PTPD) and the electron-transport layer (ETL) of phenyl-C61-butyric acid methyl ester (PCBM), as illustrated in **Fig. 8**. The modified PTPD layer, with its higher coverage and flatness, combines advantages of an appropriate work function and non-wetting surface character, and the modified PCBM with higher uniformity and lower roughness contributes to less current leakage and low charge recombination. Here we employ PEDOT:PSS as the bottom HTL because of its high conductivity, high coverage and excellent smoothness have been found by the atomic force microscope (AFM) and scanning electron microscope (SEM) images. However, the lower work function of the PEDOT:PSS relative to many other HTL materials limits the potential V_{oc} of devices. In addition, the hydrophilic surface of PEDOT:PSS tends to produce a perovskite active layer with smaller grain sizes. We demonstrated that the use of a hot substrate deposition is an effective avenue for modification of both the PTPD/PEDOT:PSS HTL and the PCBM ETL in p-i-n planar OIHP solar cells. After a simple optimization *via* this method, the V_{oc} and *PCE* were enhanced from 1.041 to 1.105 V and from 17.00 to 19.16%, respectively. With a careful and systematic study, we found that the hot substrate deposition contributes to the high coverage and low roughness of PTPD/PEDOT:PSS HTL, which can effectively mitigate the high regional series resistance and the overall lower *FF*. The modified HTL favors the formation of a higher quality perovskite film with larger grains, which indiates less charge recombination at the grain boundaries. Alternatively, hot substrate deposition method assists the formation of higher quality PCBM ETLs with improved adhesion to the perovskite surface and a more favorable surface morphology. Due to the modification of the HTL and ETL *via* the hot substrate deposition, the resulting enhancement of the V_{oc} and *PCE* of the device is evident.

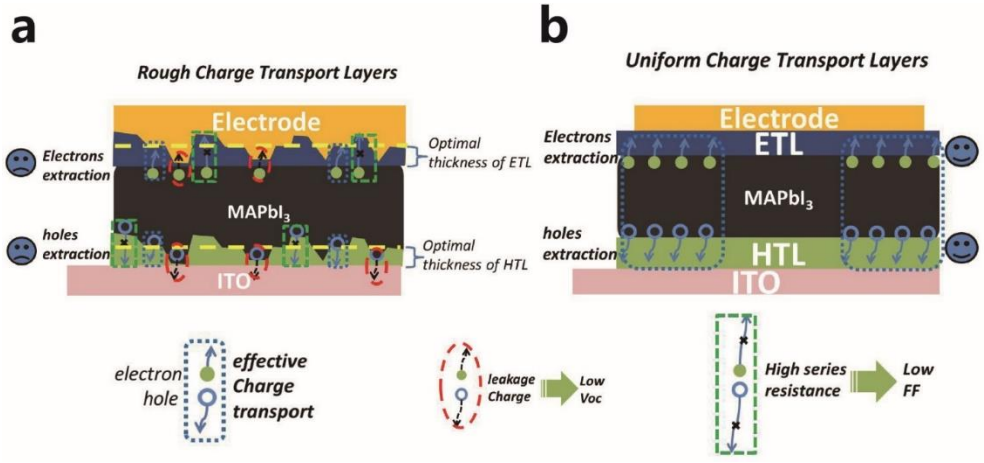

Fig. 8. a) *Charge transport in rough charge transport layers based OIHP solar cell;* ***b)*** *Charge transport in device based on charge transport layers with uniform thickness at optimal value.*

5. **Efficient Flexible Solar Cell Based On Composition-Tailored Hybrid Perovskite**

Results are published in: Cheng Bi, Bo Cheng, Haotong Wei, Stephan DeLuca, and Jinsong Huang, Efficient Flexible Solar Cell Based On Composition-Tailored Hybrid Perovskite, Adv. Mater, 29, 1605900 (2017).*

OIHPs are new photoactive layer candidates for lightweight and flexible solar cells due to their low temperature process capability, however the reported efficiency of flexible OIHP devices is far behind those achieved on rigid glass substrates. Here we reveal that the limiting factor is the different perovskite film deposition conditions required to form same film morphology on flexible substrates. An optimized perovskite film composition needs a different precursor ratio, which is found to be essential for the formation of high-quality perovskite films with longer radiative carrier recombination lifetime, smaller density of trap states, reduced precursor residue, and uniform and pin-hole free films. In this study, the flexible OHIP solar cells were fabricated on ITO-coated PET substrate with a planar heterojunction (PHJ) structure shown in **Fig. 9**a. Here, formamidinium (FA) cation was used to expand the absorption spectrum long edge of the perovskite films to 830 nm for an improved short-circuits current (J_{SC}). Methylammonium bromide (MABr, 10 wt%) was blended with FAI precursor solution to form mixed cation perovskite films for better thermal, moisture and phase stability by modifying the tolerance factor. For the perovskite solar cells made on rigid ITO/glass substrate with this composition, we obtained a high efficiency of 19.4 % and 18.8 % using the two-step interdiffusion method and one-step anti-solvent method to grow the perovskite films, respectively, as shown in **Fig. 9**b-c. Here, we used a stoichiometric molar ratio (1:1) of inorganic (PbI_2 and $PbBr_2$) and organic (FAI and MABr) precursors in one-step method. In striking contrast, the flexible device with the same deposition conditions had a significantly reduced efficiency of 9.0 %, no matter the films were made by one-step or two-step deposition methods, as shown in Figure 7b and Figure 7c. S-shape *J-V* curves were observed in almost all devices made with one-step method. The perovskite film composition was adjusted by tuning the precursor ratio to improve the film morphology and optoelectronic properties, which eventually improved the PCE to 18.1% on flexible ITO/PET substrate (**Fig. 9**d), which is a record efficiency for flexible perovskite solar cells. Our findings here point out an important direction to develop high quality perovskite films on flexible substrates by tailored composition.

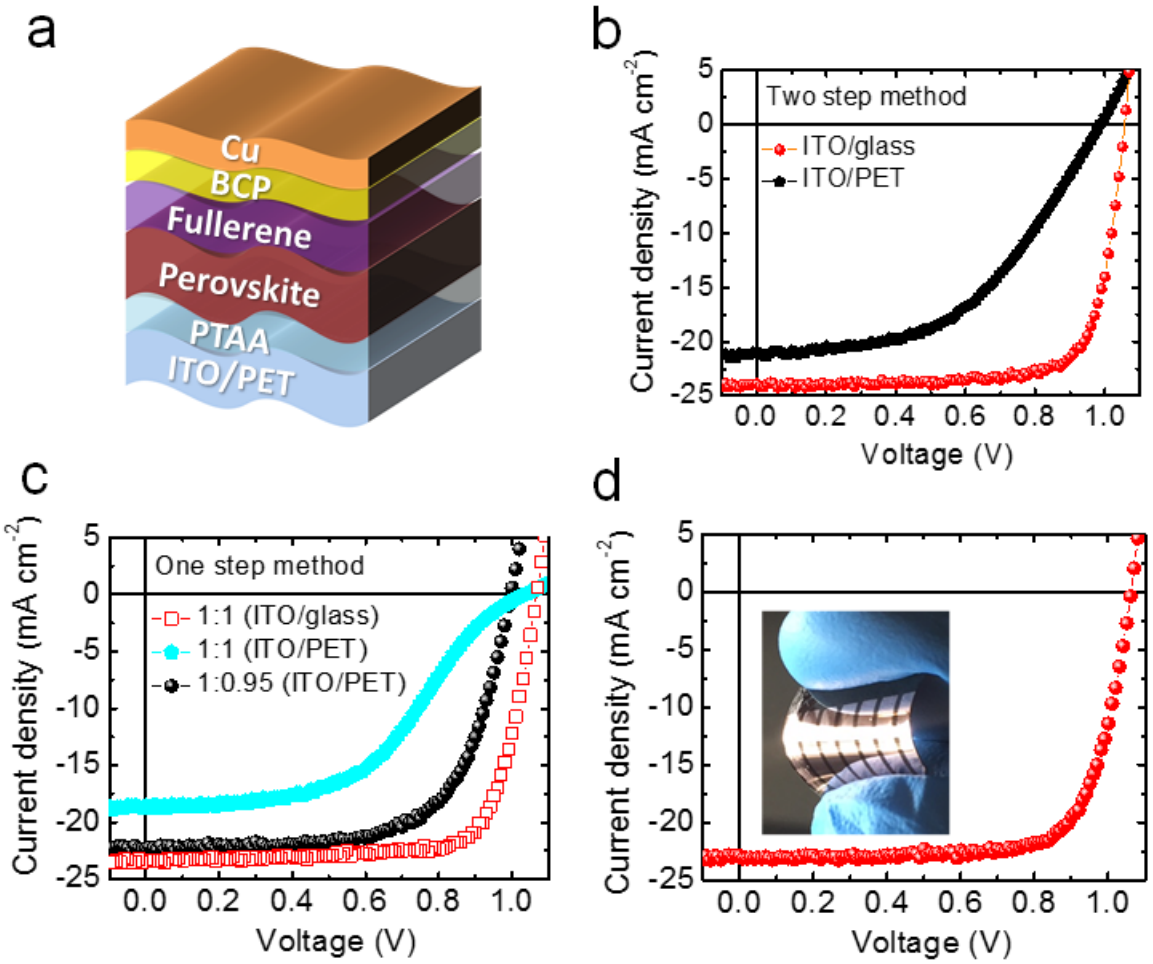

Fig. 9. *(a) Scheme of flexible OIHP device structure; (b) J-V measurement of the devices on ITO/glass and ITO/PET substrate with OIHP film grown by two-step interdiffusion method from a same deposition condition; (c) J-V curve of the devices with one-step method grown OIHP films from a stoichiometric precursor (PbI_2: FAI =1:1) on ITO/glass and ITO/PET substrate and non-stoichiometric precursor (PbI_2: FAI =1:0.95) on ITO/PET substrate; (d) J-V measurement under 1 one Sun illumination of the best-performing flexible OIHP device*

6. Spontaneous Passivation of Hybrid Perovskite by Sodium Ions from Glass Substrates

Results are published in: Cheng Bi, Xiaopeng Zheng, Bo Chen, Haotong Wei, and Jinsong Huang, Spontaneous Passivation of Hybrid Perovskite by Sodium Ions from Glass Substrates: Mysterious Enhancement of Device Efficiency Revealed, ACS Energy Lett., 2, 1400–1406 (2017).*

The efficiency of a solar cell generally decreases over time due to degradation of the devices. Here we report a spontaneous increase of device efficiency for organic–inorganic hybrid perovskite (OIHP) solar cells after a period of storage that is speculated to be related to the sodium

ions (Na^+) diffused from the substrate. The efficiency of a p–i–n planar heterojunction structure device rises from 18.8 to 20.2% (**Fig. 10**) after 24 h of storage in nitrogen. The increased efficiency can be explained by the prolonged carrier lifetime and reduced trap density in the OIHP films. The expected contribution by Na^+ in defect passivation has been evidenced by studying the evolution of the film's photoluminescence (PL) lifetime, trap density, and device efficiency over storage duration on varied substrates that either contain Na+ or do not. The passivation effect of Na^+ is further identified by the improved PL lifetime observed in the OIHP film made on a silicon substrate with intentionally added Na^+.

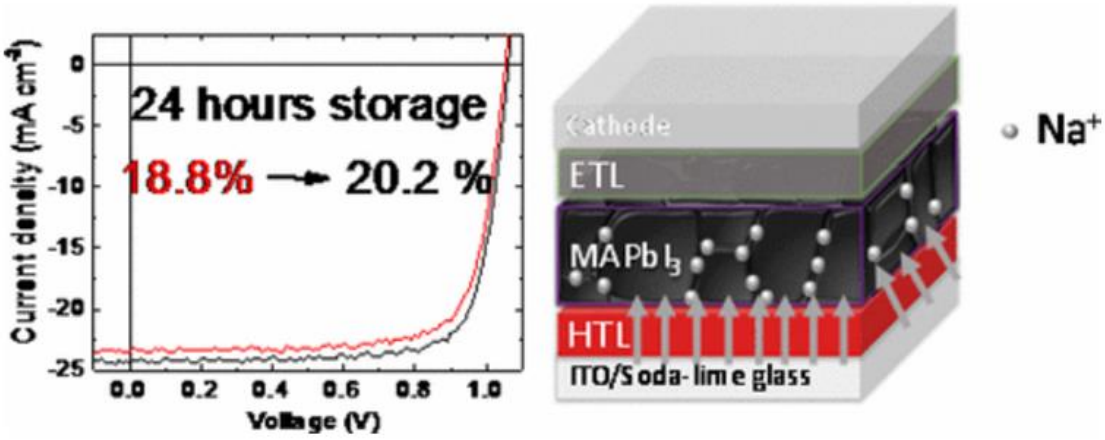

***Figure 10**. Efficiency of a p–i–n planar heterojunction structure device before and after 24 h of storage in nitrogen.*

7. Dual-function of Crystallization Controlling and Defect Passivation enabled by Sulfonic Zwitterion

Results are published in: Dual-function of Crystallization Controlling and Defect Passivation enabled by Sulfonic Zwitterion for Stable and Efficient Perovskite Solar Cells, Xiaopeng Zheng, Yehao Deng, Shi Tang , Yanjun Fang, Qi Wang, Yuze Lin, Yang Bai, Xun Xiao, Zhenhua Yu, Ye Liu, Haotong Wei, Chen Bo, and Jinsong Huang, **Advanced Materials**, 30, 1803428, 2018*

Previous we mainly use 3-(decyldimethylammonio)-propane-sulfonate inner salt (DPSI) for surface passivation. Here we explore using DPSI, which is a sulfonic zwitterion, to passivate the grain boundaries. To achieve that, we added DPSI into the solution of perovskites. It is shown that the DPSI plays dual roles in tuning the crystallization behavior and passivating the defects of perovskites, as illustrated in Figure 11. The synergistic effect of crystallization control and defect passivation remarkably suppresses pinhole formation, reduces the charge trap density, and lengthens the carrier recombination lifetime, and thereafter boosts the small-area (0.08 cm2) planar perovskite device efficiency to 21.1% and enables a high efficiency of 18.3% for bladecoating large-area (1 cm2) devices. The device also shows good light stability, which remains at 88% of the initial efficiency under continuous unfiltered AM 1.5G light illumination

for 480 h. These findings provide an avenue for simultaneous crystallization control and defect passivation to further improve the performance of perovskite devices.

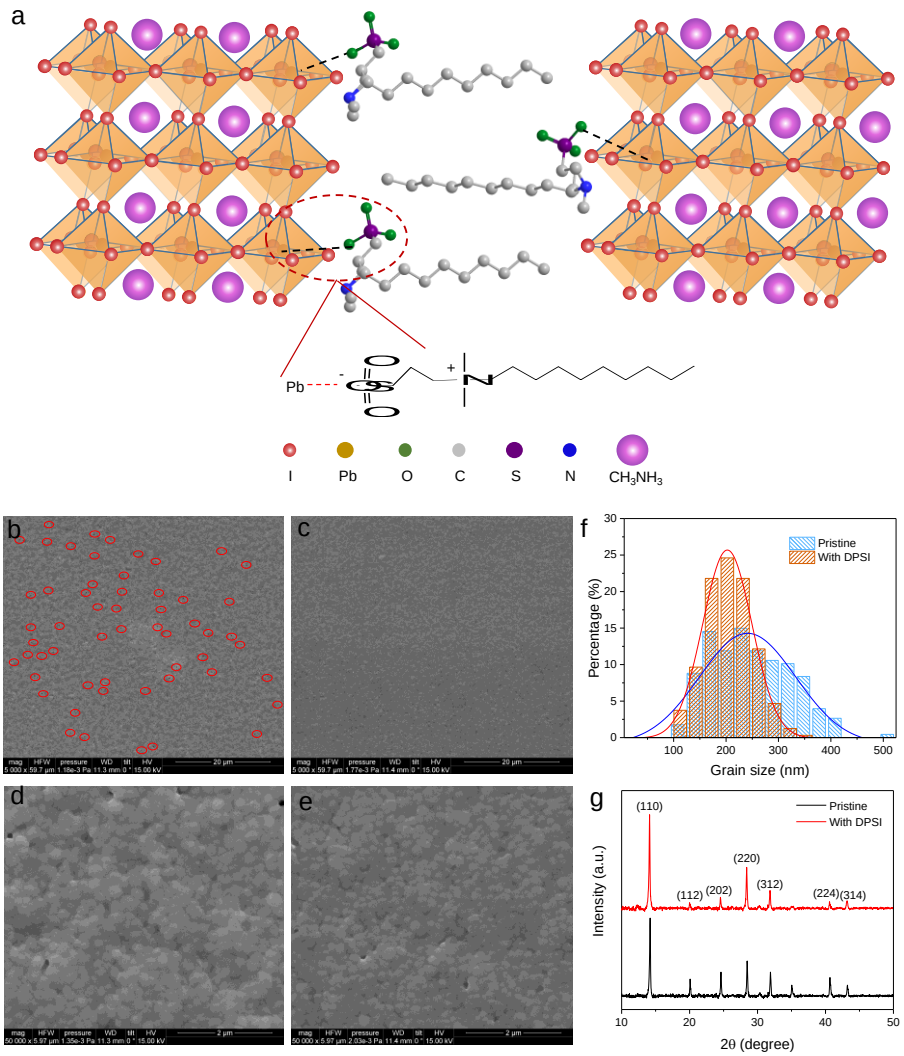

Figure 11. DPSI mediate perovskite thin film growth. a, Schematic illustration of DPSI mediate the perovskite growth and defect passivation. The DPSI molecules firstly attached on the surface of perovskite nucleus and precise control each grain growth to uniform size. Then the DPSI molecules were repelled to the grain boundaries and film surfaces after the perovskite film formation and passivate the defect states at grain boundaries and film surfaces. b and c, Scanning electron microscopy (SEM) images of the MAPbI3 films without and with adding of the DPSI molecules, respectively. The pin-holes are marked with the red circles. d and e, The enlarged SEM images of the MAPbI3 films without and with adding of the DPSI molecules, respectively. f, Grain size distributions calculated from ~300 grains from the SEM images. Blue and red solid lines represent the Gaussian distribution fitting for the statistics of grain size. g, XRD patterns of pristine MAPbI3 film and the film with DPSI.

8. Bilateral alkylamine to reinforce the grain boundaries

Results are published in: Bilateral alkylamine for suppressing charge recombination and improving stability in blade-coated perovskite solar cells, Wu-Qiang Wu, Zhibin Yang, Peter N. Rudd, Yuchuan Shao, Xuezeng Dai, Haotong Wei, Jingjing Zhao, Yanjun Fang, Qi Wang, Ye Liu, Yehao Deng, Xun Xiao, Yuanxiang Feng, Jinsong Huang, **Science Advances**, 5, 3, eaav8925 2019*

The power conversion efficiencies of perovskite solar cells are already higher than that of other thin film technologies, but laboratory cell-fabrication methods are not scalable. Here, we report an additive strategy to enhance the efficiency and stability of PSCs made by scalable blading. Blade-coated PSCs incorporating bilateral alkylamine (BAA) additives achieve PCEs of 21.5 (aperture, 0.08 cm^2) and 20.0% (aperture, 1.1 cm^2), with a record-small open-circuit voltage deficit of 0.35 V under AM1.5G illumination. The stabilized PCE reaches 22.6% under 0.3 sun. As illustrated in Fig. 12, simple tailoring of the perovskite ink formulation with a small amount of bilateral alkylamine (BAA) additive, i.e., molecules with a structure of "NH2–R–NH2," not only helps in constructing compact perovskite films with uniform size distribution and fewer pinholes but also has strong capability to passivate the perovskite grain surface. In addition, the BAA molecules link neighboring grains and enforce them. Anchoring monolayer bilateral amino groups passivates the defects at the perovskite surface and enhances perovskite stability by exposing the linking hydrophobic alkyl chain. Grain boundaries are reinforced by BAA and are more resistant to mechanical bending and electron beam damage. BAA improves the device shelf lifetime to >1000 hours and operation stability to >500 hours under light, with 90% of the initial efficiency retained.

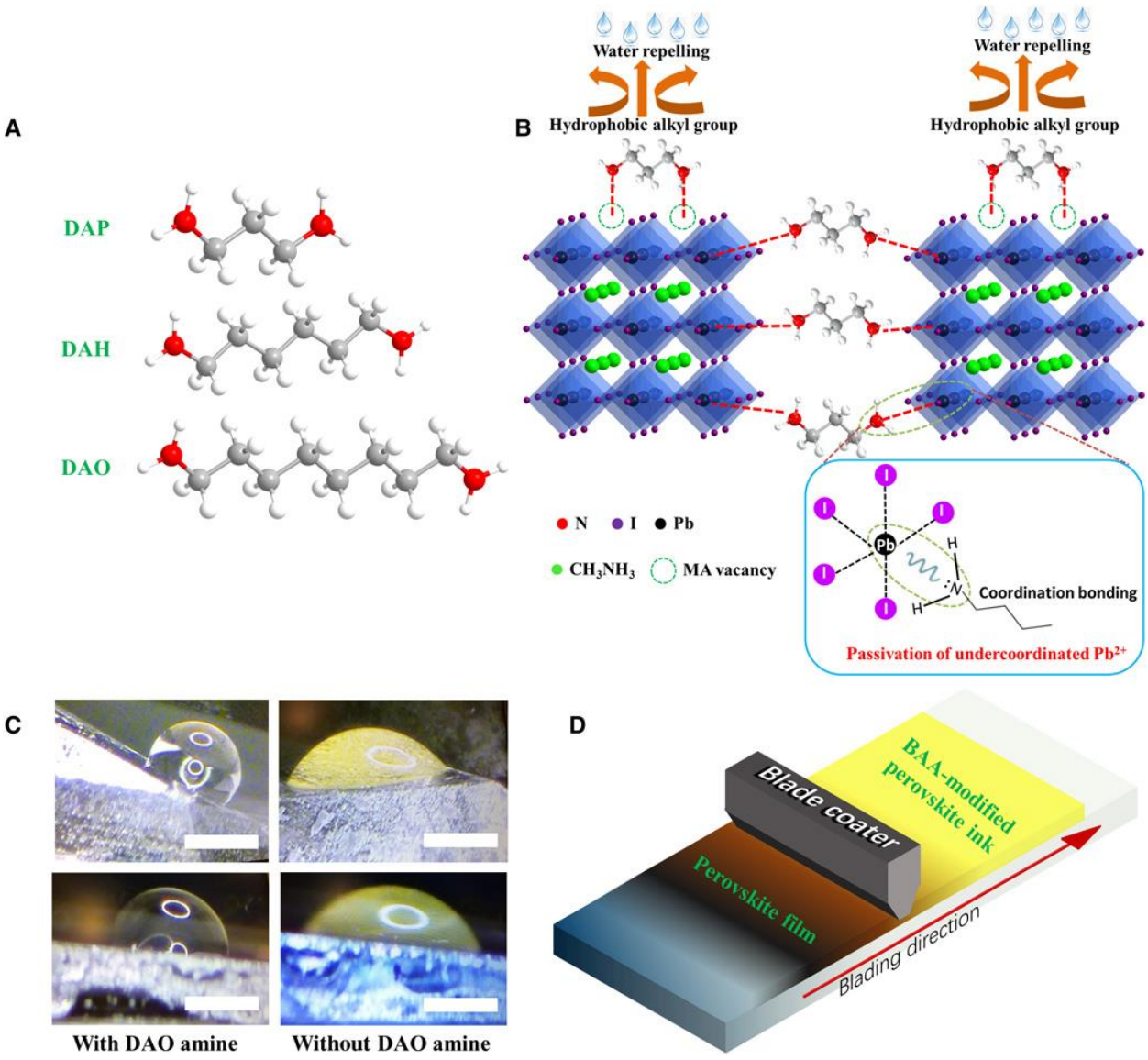

Fig. 12 Chemical structures and functions of BAA additives, contact angle measurement, and blading process. (A) Chemical structures of BAA additives. (B) Schematic illustration of defect passivation and water repellence induced by BAA incorporation. (C) Contact angle measurement of a water droplet on MAPbI3 single crystals (top row) and MAPbI3 thin films (bottom row) with or without incorporated BAA additive. Scale bars, 5 cm. (D) Sketch showing the blade-coating process for the perovskite film.

9. Molecular tuning of passivation molecules

Results are published in: Tailoring Passivation Molecular Structures for Extremely Small Open Circuit Voltage Loss in Perovskite Solar Cells, Shuang Yang, Jun Dai, Zhenhua Yu, Charles H Van Brackle, Yuchuan Shao, Yu Zhou, Xun Xiao, Xiao Cheng Zeng and Jinsong Huang,* ***Journal of the American Chemical Society,*** *141,14, 5781-5787, 2019*

Passivation of electronic defects at the surface and grain boundaries of perovskite materials has become one of the most important strategies to suppress charge recombination in both polycrystalline and single crystalline perovskite solar cells. Although many passivation molecules have been reported, it remains very unclear on the passivation mechanisms of various functional groups. Here, we systematically engineer the structures of passivation molecular functional groups, including carboxyl, amine, isopropyl, phenethyl and tert-butyl-phenethyl groups, and study their passivation capability to perovskites. It reveals the carboxyl and amine groups would heal charged defects via electrostatic interactions, and the neutral iodine related defects can be reduced by the aromatic structures. The judicious control of the interaction between perovskite surface and molecules can further realize the grain boundary passivation, including those are deep toward substrates. As illustrated in Fig. 13, the passivation of phenyalanine is the sum of passivation effect of phenypropionic acid and phenethylamine, because it has both function group of these two. Understanding of the underlining mechanisms allows us to design a new passivation molecule, D-4-tert-butyl-phenylalanine, yielding high-performance p-i-n structure solar cells with a stabilized efficiency of 21.4%. The open-circuit voltage of a device with perovskite optical bandgap of 1.57 eV reaches 1.23 V, corresponding to a record low V_{OC} deficit of 0.34 V at the time of publication. This findings provide a guidance for future design of new passivation molecules to realize multiple facets applications in perovskite electronics.

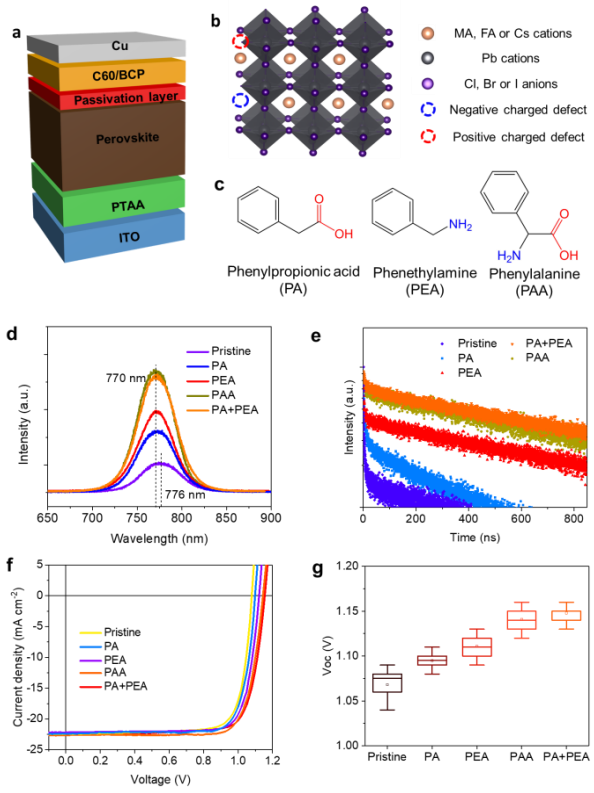

Figure 13. (a) The device structure of perovskite planar heterojunction solar cells. (b) Schematic illustration of surface charged defects. (c) Chemical structure of passivation molecules with

marked amino (blue) and carboxyl (red) groups. (d) PL and (e) TRPL spectra of perovskite films with different passivation layers. (f) J-V curves and (g) statistics of VOC distribution of perovskite solar cells with different passivation layers.

10. Conversion of surface into oxide for passivation and stabilization

*Results are published in: Stabilizing halide perovskite surfaces for solar cell operation with wide-bandgap lead oxysalts, Shuang Yang, Shangshang Chen, Edoardo Mosconi, Yanjun Fang, Xun Xiao, Congcong Wang, Yu Zhou, Zhenhua Yu, Jingjing Zhao, Yongli Gao, Filippo De Angelis, Jinsong Huang, **Science**, Vol. 365, Issue 6452, pp. 473-478, 2019*

Four years ago, we proposed the concept of passivation using organic molecules for the first time which is now broadly accepted. We want to point out it is fundamentally different from the passivation techniques in silicon solar cells where oxide or nitride passivation layers forming primary chemical bonding with silicon are important to protect silicon in addition to reducing surface dangling bonds. Here we report to do something similar in the passivation of perovskite solar cells by developing an inorganic passivation layer on perovskites which is mechanically strong, compact, and chemically stable with wide band gap.

Here we demonstrate a generic strategy to form a thin and water-insoluble Pb-oxysalt layer on the surface of perovskite material by converting top surface of perovskite to Pb-oxysalt. These oxysalt thin layers enhance the resistance of the perovskite films to the attacking of environmental hazards (moisture, oxygen) due to the formation of strong chemical bonding. The Pb-oxysalt layers also reduce the surface defect density by reaction with defective sites, in addition to the passivation effect due to the wide bandgap. The concept is illustrated in **Fig. 14a**, w converted the surface of perovskites by exposing it to oxysalt solution, The formed lead sulfate has very low solubility in water. The formation of a conformal and condensed layer effectively stops moisture permeation. In addition, the wide bandgap lead sulfate also effectively reduce charge recombination, similar to the function of silicon oxide on silicon. The Pb-oxysalt layers elongates the carrier recombination lifetime, and improves the efficiency of the solar cells to 21.1%. Encapsulated solar cell devices based on triple cations perovskites maintain 96.8% of the initial efficiency after operation at maximum power point under simulated AM 1.5G irradiation for 1200 hours at 65 °C, which represents a record stability for perovskite solar cells. This work is original and demonstrates for the first time of passivation methodology of perovskite-based devices that is comparable to the well-developed silicon photovoltaics.

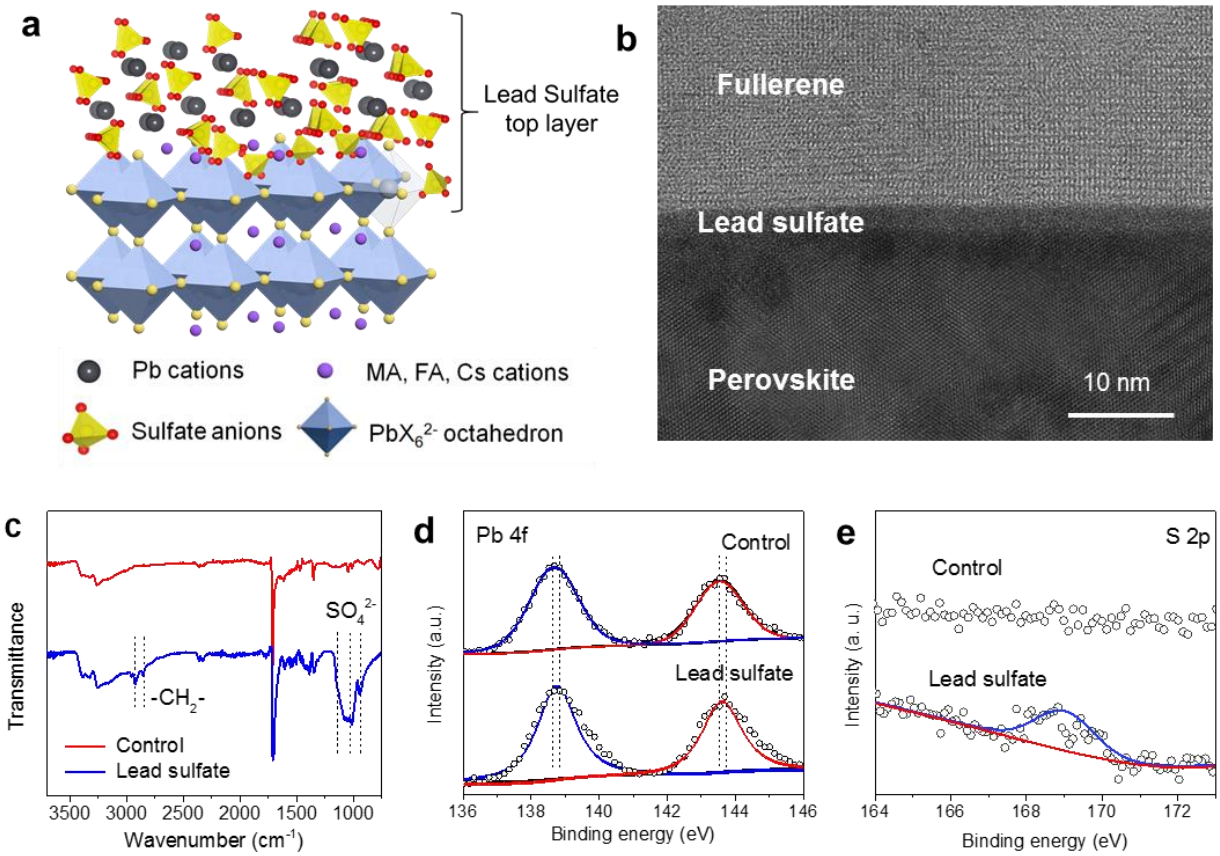

Fig. 14. Organohalide lead perovskite stabilized by a lead sulfate surface layer. (a) Schematic illustration of protection of perovskites by in-situ formation of a lead sulfate top layer on the perovskite surface. (b) Cross-sectional HR-TEM image of the perovskite/lead sulfate layer/C60 interface. (c) FT-IR measurement of perovskite powder with or without the lead sulfate layer. The XPS spectra of Pb 4f (d) and S 2p (e) for the perovskite films deposited on ITO glass.

11. Strengthen surface bonding to reduce iodine deficiency

Results are published in: Reducing Surface Halide Deficiency for Efficient and Stable Iodide-Based Perovskite Solar Cells, Wu, Wu-Qiang; Rudd, Peter; Ni, Zhenyi; Van Brackle, Charles; Wei, Haotong; Wang, Qi; Ecker, Benjamin; Gao, Yongli; Huang, Jinsong, ***Journal of the American Chemical Society*** *, 142, 8, 3989-3996, 2020*

State-of-the-art, high-performance perovskite solar cells contain a large amount of iodine to realize smaller bandgaps. However, the presence of numerous iodine vacancies at the surface of the film formed by their evaporation during the thermal annealing process has been broadly shown to induce deep-level defects, incur nonradiative charge recombination, and induce photocurrent hysteresis, all of which limit the efficiency and stability of PSCs. In this work, modifying the defective surface of perovskite films with cadmium iodide (CdI_2) effectively reduces the degree of surface iodine deficiency and stabilizes iodine ions via the formation of strong Cd–I ionic bonds,

as illustrated in **Fig. 15**. This largely reduces the interfacial charge recombination loss, yielding a high efficiency of 21.9% for blade-coated PSCs with an open-circuit voltage of 1.20 V, corresponding to a **record small voltage deficit of 0.31 V**. The CdI_2 surface treatment also improves the operational stability of the PSCs, retaining 92% efficiency after constant illumination at 1 sun intensity for 1000 h. This work provides a promising strategy to optimize the surface/interface optoelectronic properties of perovskites for more efficient and stable solar cells and other optoelectronic devices.

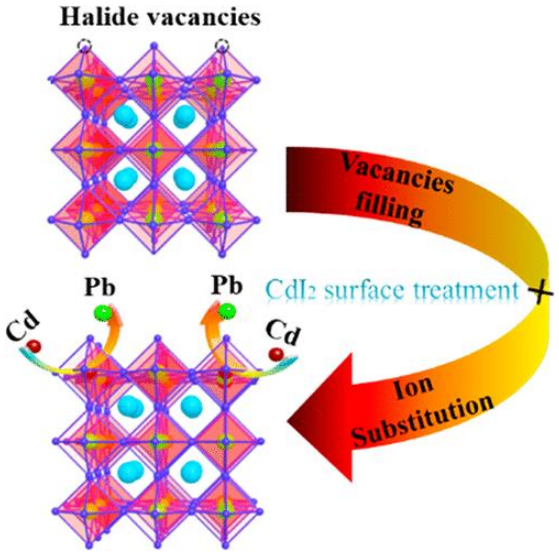

Fig.15 Illustration of stabilization of perovskite surface using stronger Cd-I bonding

III. Publications

1. Reducing Surface Halide Deficiency for Efficient and Stable Iodide-Based Perovskite Solar Cells, Wu, Wu-Qiang; Rudd, Peter; Ni, Zhenyi; Van Brackle, Charles; Wei, Haotong; Wang, Qi; Ecker, Benjamin; Gao, Yongli; Huang, Jinsong, **Journal of the American Chemical Society** , 142, 8, 3989-3996, 2020
2. Stabilizing halide perovskite surfaces for solar cell operation with wide-bandgap lead oxysalts, Shuang Yang, Shangshang Chen, Edoardo Mosconi, Yanjun Fang, Xun Xiao, Congcong Wang, Yu Zhou, Zhenhua Yu, Jingjing Zhao, Yongli Gao, Filippo De Angelis, Jinsong Huang, **Science**, Vol. 365, Issue 6452, pp. 473-478, 2019
3. Imperfections and their passivation in halide perovskite solar cells Chem. Soc. Rev. Bo Chen, Peter N. Rudd, Shuang Yang, Yongbo Yuan and Jinsong Huang*, **Chemical Society Reviews**, 48, 3842-3867, 2019
4. Tailoring Passivation Molecular Structures for Extremely Small Open Circuit Voltage Loss in Perovskite Solar Cells, Shuang Yang, Jun Dai, Zhenhua Yu, Charles H Van Brackle, Yuchuan Shao, Yu Zhou, Xun Xiao, Xiao Cheng Zeng and Jinsong Huang*, **Journal of the American Chemical Society,** 141,14, 5781-5787, 2019

5. Bilateral alkylamine for suppressing charge recombination and improving stability in blade-coated perovskite solar cells, Wu-Qiang Wu, Zhibin Yang, Peter N. Rudd, Yuchuan Shao, Xuezeng Dai, Haotong Wei, Jingjing Zhao, Yanjun Fang, Qi Wang, Ye Liu, Yehao Deng, Xun Xiao, Yuanxiang Feng, Jinsong Huang*, **Science Advances**, 5, 3, eaav8925 2019
6. Dual-function of Crystallization Controlling and Defect Passivation enabled by Sulfonic Zwitterion for Stable and Efficient Perovskite Solar Cells, Xiaopeng Zheng, Yehao Deng, Shi Tang , Yanjun Fang, Qi Wang, Yuze Lin, Yang Bai, Xun Xiao, Zhenhua Yu, Ye Liu, Haotong Wei, Chen Bo, and Jinsong Huang*, **Advanced Materials**, 30, 1803428, 2018
7. Intrinsic Behavior of CH3NH3PbBr3 Single Crystals under Light Illumination, Benjamin R. Ecker , Congcong Wang, Haotong Wei, Yongbo Yuan, Jinsong Huang and Yongli Gao, **Advanced Materials Interface**, 5, 23,1801206 (2018)
8. Argon plasma treatment to tune perovskite surface composition for high efficiency solar cells and fast photodetectors, Xun Xiao, Chunxiong Bao, Yanjun Fang, Jun Dai, Benjamin R. Ecker, Yuze Lin, Shi Tang, Ye Liu, Yehao Deng, Xiaopeng Zheng, Yongli Gao, Xiao Cheng Zeng and Jinsong Huang, **Advanced Materials**, 2018,
9. Zhenhua Yu, Linxing Zhang, Sen Tian, Fan Zhang, Bin Zhang, Fangfang Niu, Pengju Zeng, Junle Qu, Peter Rudd, Jinsong Huang* and Jiarong Lian, Hot-substrate Deposition of Hole and Electron Transport Layers for Enhanced Performance in Perovskite Solar Cells, **Advanced Energy Materials**, 2017
10. Advance in Understanding the Physical Properties of Hybrid Perovskites for Photovoltaic Applications, Jinsong Huang, Yongbo Yuan, Yuchuan Shao and Yanfa Yan, **Nature Materials Reviews**, 2017
11. Xiaopeng Zheng, Bo Chen, Jun Dai, Yanjun Fang, Yang Bai, Yuze Lin, Haotong Wei, Xiao Cheng Zeng and Jinsong Huang*, Defect Passivation using Quaternary Ammonium Halides for High Efficiency Perovskite Solar Cells, **Nature Energy**, 2, 17102 (2017)
12. Efficient Flexible Solar Cell Based On Composition-Tailored Hybrid Perovskite, Cheng Bi, Bo Chen, Haotong Wei, Stephan DeLuca, and Jinsong Huang, **Advanced Materials**, 2017
13. Spontaneous Passivation of Hybrid Perovskite by Sodium Ions from Glass Substrates-Mysterious Enhancement of Device Efficiency Revealed Bi, Cheng; Zheng, Xiaopeng; Chen, Bo; Wei, Haotong; Huang, Jinsong, **ACS Energy Letters**, 2, 1400-1406, 2017
14. The Functions of Fullerenes in Hybrid Perovskite Solar Cells, Y. Fang, C. Bi, D. Wang, and J. Huang, **ACS Energy Letters**, 2,782-794,2017